

RESEARCH ARTICLE

Ensemble Learning With Symbiotic Organism Search Optimization Algorithm for Breast Cancer Classification and Risk Identification of Other Organs on Histopathological Images

NALINIKANTA ROUTRAY¹, SAROJA KUMAR ROUT², BANDITA SAHU¹,
SANDEEP KUMAR PANDA³, AND DEEPTHI GODAVARTHI⁴

¹Department of Computer Science and Engineering, GIET University, Gunupur, Odisha 765022, India

²Department of Information Technology, Vardhaman College of Engineering (Autonomous), Hyderabad, Telangana 501218, India

³Department of Artificial Intelligence and Data Science, Faculty of Science and Technology (IcfaiTech), ICFAI Foundation for Higher Education, Hyderabad, Telangana 500029, India

⁴School of Computer Science and Engineering (SCOPE), VIT-AP University, Amaravati, Andhra Pradesh 522237, India

Corresponding author: Sandeep Kumar Panda (sandeepkumar@ifheindia.org)

This work was supported in part by the Faculty of Science and Technology (IcfaiTech), and in part by the ICFAI Foundation for Higher Education, Hyderabad, Telangana, India.

ABSTRACT Breast cancer (BC) is closely linked with the maximum mortality rate for cancer detection across the globe and has become a predominant public health issue. Earlier detection might increase the possibility of survival and successful treatment. However, it is a time-consuming and very challenging task that depends on the diagnostician's experience. For patients and their prognosis, it is essential that BC cancer can be automatically detected by the analysis of histopathological images. Conventional feature extraction method extracts some lower-level features of images, and preceding knowledge is essential for selecting suitable features that could be heavily impacted by human beings. The deep learning (DL) technique extracts higher-level abstract features from an image automatically. Therefore, this study develops a new Ensemble Learning with Symbiotic Organism Search Optimization Algorithm for Breast Cancer Classification (ELSOSA-BCC) technique on Histopathological Images. In the ELSOSA-BCC technique, the noise is removed using Gabor filtering (GF). In addition, the ELSOSA-BCC technique employs the EfficientNet-B0 model for feature extraction and optimal hyperparameter tuning using the SOS algorithm. Finally, the ensemble learning-based classification process is performed by three classifiers namely deep stacked autoencoder (DSAE), kernel extreme learning machine (KELM), and bidirectional long short-term memory (BiLSTM). In this study, ELSOSA-BCC simulation values are tested on a medical dataset. ELSOSA-BCC has been shown to perform better than other models in the experimental results.

INDEX TERMS Medical imaging, breast cancer, ensemble learning, deep learning, histopathological images.

I. INTRODUCTION

Breast cancer (BC) is the major factor in higher mortality rates in women all around the world. The heterogeneous nature of BC makes its initial representation a crucial step in treatment planning and decision-making [1]. The routine clinical analysis of BC can be performed by using several

radiology images, involving Magnetic Resonance Imaging (MRI), ultrasound, and mammography. Nonetheless, this non-invasive methodology might not effectively represent the heterogeneous behavior of BC [2]. Hence, the pathological study is followed as a benchmark to comprehend the pathophysiology of BC. In the presented technique, the tissue sample is collected and mounted on glass slides and then stained this slide for the best description of immunophenotypic and tumoral morphological features [3].

The associate editor coordinating the review of this manuscript and approving it for publication was Chao Zuo¹.

Later, pathologists proceed with the microscopic analysis of this slide to conclude a potential diagnosis of BC. Conversely, the manual interpretation of histopathology images could be a time-consuming and challenging task and might lead to biased results [4].

The diagnostic method of BC is operator-dependent and needs a skilled physician. However, some human factors like insufficient concentration and exhaustion might cause the misdiagnosis of sample types within continuous and long processes [5]. In case of misdiagnosis, cancer might grow, and the survival rate becomes lower. Few countries have a low number of diagnosticians per population [6]. To counteract the possibility of error, the lack of skilled pathologists, the laborious process, the high cost, and many Computer-Aided Diagnosis (CAD) methods for automatic and early diagnosis of BC were introduced and assessed by researcher workers in the past. This technique could considerably assist in the earlier detection of cancer. But it is difficult to enforce [7]. With the increase of deep learning (DL) (as an integral component of the ML family), many researchers have applied this technique to accurately determine sample types in histology images. However, the complicated structure of human body cells [8], low image quality, and comparison among benign and malignant samples from one side and the various cell scales, sizes, shapes, and colors in the histological image from the other side can make the task most complex and prevent accomplishing higher accuracy.

In addition, the lack of labeled and extensive datasets has made another serious problem for the abovementioned challenges [9]. In the context of DL, features can be extracted and retrieved data automatically, and abstract representations can be learned automatically. In the fields of biomedical science, computer vision, etc., they could solve the problem of conventional feature extraction [10]. Parallel to this, the unprecedented advances in machine learning enable diagnosis based on image analysis, previously only possible in certain specialties, through the synergy of artificial intelligence and digital pathology. In comparison with human pathologists evaluating options, computer-aided image analysis allows for a more thorough identification, extraction, and quantification of features [11]. An artificial intelligence-based diagnosis of skin cancer is compared with datasets widely used and prevalent reviews. Using deep learning and machine learning techniques, the research will provide a deeper understanding of skin cancer diagnosis [12]. The tumor-associated microbiota has been studied in several ways to date, shedding light on its composition, function, and clinical relevance. It is imperative to approach tumor-associated microbiota studies from a holistic perspective, taking into account the technical, analytical, biological, and clinical challenges [13]. An ultrasound image classification framework that integrates deep learning and metaheuristic optimization is described in this research work [14]. This is an algorithm for constructing an efficient neural network architecture that uses Bayesian convolutional neural architectures and

Gaussian processes to detect and classify colon and lung cancers more efficiently [15].

Breast cancer has the potential to spread to various body regions through a process known as metastasis. Detecting associated risks requires a comprehensive approach involving diagnostic imaging, medical history review, and clinical assessment. Advanced imaging techniques like CT, PET, and MRI scans play a crucial role in identifying metastatic sites such as the lungs, liver, bones, and brain. Additionally, a thorough evaluation of a patient's medical history and symptoms is essential for assessing potential vulnerabilities. For example, breast cancer metastasizing to the bones can result in fractures, bone pain, and compression of the spinal cord. Liver metastases may lead to symptoms like jaundice, abdominal pain, and compromised liver function. Lung metastases could manifest as respiratory difficulties, persistent cough, and chest discomfort. Identifying risks associated with other organs affected by breast cancer is critical for devising effective treatment strategies. Highlighting the importance of early detection, accurate diagnosis, and a comprehensive approach to addressing metastases is paramount. These factors collectively contribute to minimizing the impact on other organs and enhancing the overall quality of life for patients.

ELSOSA-BCC is a new technique of ensemble learning with symbiotic organisms search optimization applied to histopathological images for the classification of breast cancer. As part of the noise removal process, ELSOSA-BCC implements Gabor filtering (GF). In addition, the ELSOSA-BCC technique employs the EfficientNet-B0 model for feature extraction and optimal hyperparameter tuning using the SOS algorithm. Finally, the ensemble learning-based classification process is performed by three classifiers namely deep stacked autoencoder (DSAE), kernel extreme learning machine (KELM), and bidirectional long short-term memory (BiLSTM). The main goal of breast cancer prediction is to determine and evaluate the likelihood that the disease will develop or recur. However, it's important to keep in mind that there may be potential hazards or factors involving other organs or components of the patient's health. It is critical to determine whether individuals receiving therapy for breast cancer are at risk for heart-related issues or illnesses. Breast cancer treatments, especially hormonal ones, can lower bone density and raise the risk of fractures or osteoporosis. Fertility preservation and potential effects on reproductive health should be taken into account for younger women with breast cancer. It can be easier to spot the dangers of infections or other immune-related problems if you are aware of how breast cancer and its therapies may affect your immune system. Breast cancer hormone therapy can affect the endocrine system, which could have adverse effects or long-term repercussions on multiple organs. Future development of other cancers may be more likely for patients with breast cancer. For long-term health management, this risk must be recognized and addressed.

Cancer image datasets can be analyzed using the ELSOSA-BCC optimization technique, which includes feature selection, parameter optimization, and model tuning in machine learning and data analysis. It is based on the symbiotic relationship that two or more species have in nature, where their existence benefits both. Complex optimization problems are frequently solved using the ELSOSA-BCC optimization technique. The premise behind ensemble learning is that by combining the results of several different models, the strengths of the individual models can make up for the deficiencies of the other models, resulting in a more precise and reliable final prediction.

The application of Ensemble Learning with Symbiotic Organism Search Optimization Algorithm (ELSOSA) in Breast Cancer Classification and Risk Identification carries substantial implications in healthcare. This method enhances breast cancer detection by combining diverse classifiers and optimizing hyperparameters, thereby reducing diagnostic errors. Early-stage identification through ELSOSA enables timely interventions, potentially improving treatment outcomes. Medical professionals benefit from precise risk assessment and classification, facilitating personalized treatment plans and expediting decision-making. The model's transparency and interpretable hyperparameters are still confident in its predictions.

In a broader healthcare context, ELSOSA's implementation can optimize resource allocation and reduce healthcare facility strain. Accurate classification aids in efficient resource distribution, focusing on high-risk patients. ELSOSA promises benefits for patients, medical practitioners, and the healthcare system. It enhances breast cancer classification and risk assessment accuracy, translating to improved patient well-being, streamlined resource distribution, and advancements in diagnostic techniques beyond breast cancer.

A medical dataset can be used to test ELSOSA-BCC simulation values. The research work also emphasizes how breast cancer affects other organs quickly. Other body parts can be affected by breast cancer, resulting in additional symptoms. Lymph nodes under the arm are often the first detectable sites of cancer dissemination, even if they are cancer-bearing lymph nodes that cannot be touched. Malignant cells can metastasize to the lungs, liver, brain, and bones. Additionally, bone pain and headaches can manifest if they reach these locations.

II. RELATED WORKS

In [16], presented a DL and TL-related method for classifying histopathological imageries for BC diagnosis. A patch selection method was implemented using TL without performance losses for classifying breast histopathologic images. At first, the extraction of patches will be done from Whole Slide Images (WSI) and given to CNN for extracting the feature. To train an SVM classifier, Features from the Efficient-Net structure were used. Based on histopathologic images, the authors developed a hybrid DNN to recognize cancer at

the image level [17]. The hybrid DNN includes residual block and inception. The network incorporated an advanced multi-level feature map for histopathologic imageries and included the boon of residual and inception blocks. The method combined the strength of residual and inception blocks and displays the stability in performance against current methods. Deep learning applications in translational bioinformatics, medical imaging, pervasive sensors, medical informatics, and public health are emphasized in the paper. It provides a critical analysis of the relative merits, potential pitfalls, and prospects of deep learning in health informatics as well as a comprehensive overview of current research [18]. As machine learning (ML) became easier and deeper learning (DL) became more accurate, image classification became much easier. A hybrid deep learning (HDL) model combines two or more deep learning architectures. In several applications, HDL models are becoming popular. However, these applications have not been reviewed [19]. The organic characteristics of brain tumors make them difficult to treat, to a great extent as a result of their restricting effects on progress. Machine Learning and Image Processing algorithms can be used to detect tumors [20]. To predict critical and non-critical cases, a binary version of the Whale Optimization Algorithm (WOA) was developed. It identifies minimally optimal features while maximizing classification accuracy by using sigmoid transfer functions [21]. The problem can be solved by using artificial jellyfish search optimization (JS) algorithms in combination with artificial neural networks (ANN). Using JellyfishSearch_ANN, the research work derived the algorithm, that classifies cervical cancer data with four types of targets [22]. Based on baseline FDG-PET scans, lymphoma lesions can be segmented and prognosis predictions can be made for patients with diffuse large B-cell lymphoma (DLBCL). The vast size and diffusely arranged lymphoma cells of DLBCL, as well as the extremely heterogeneous nature of the group of neoplasms that it belongs to, make the duties difficult [23].

Burçak et al. [24] devised a deep CNN method. The technique utilizes several methods (i.e., RMSprop, stochastic gradient descent, adaptive gradient, Adam, AdaDelta, and Nesterov accelerated gradient) for computation of the primary weight of the network and upgrades the model variables for faster BP learning. The authors have used the parallel computing structure with Cuda-based graphics processing units so that the model can be trained with less hardware in a short period. The author [25] introduced a novel hybrid convolutional and recurrent DNN for BC histopathologic image classification. Depending on richer multi-level feature representations of the histopathologic image patches, this technique integrated the merits of convolution and RNN, and long-term and short-term spatial correlation among patches are conserved [26]. A method for detecting sepsis early on, using support vector machines (SVMs) and long short-term memories (LSTMs), is described in [27]. Zeiser et al. [28] modeled a method that relies upon CNN to offer a refined and multiclass segmentation of WSI for BC. Such modules

were prearranged for decoding the data learned through CNNs in interpretable estimation for diagnosticians. The pre-processing module can be accountable for eliminating the background and noise of WSI. At ROI recognition, the authors used the U-Net convolutional structure to find suspicion low magnification WSI. In [29], the authors modeled a new DL model formulated depending on a CNN. The success of the classification has been raised through the presented technique called opposed as BreastNet. The BreastNet method was based on an attention module-based residual architecture. Every images image data will be processed through the augmented methods before applying it as input to the model. In [30], the authors proposed 2 mechanisms for diagnosing BC from multi- and single-magnification histopathologic images. The first provided mechanism uses a pre-trained DenseNet201 CNN structure and optimally tunes over widely accessible BreakHis datasets and classifies histopathologic imageries of particular magnification elements into one of the malignant or benign classes [31], [32], [33].

The study concentrated on pixel-level semantic segmentation of breast lesions using ultrasonic images. It incorporated dilated factors in segmentation and used ultrasonic imaging masks for the dataset. After segmentation, an erosion and size filter removed noise, enhancing alignment with ground truth masks [46]. The article aims to tackle these concerns with a novel TTCNN-based breast cancer detection method. It involves extracting deep features from eight DCNN models and selecting optimal layers based on classification performance, enhancing effectiveness [47]. This study presents a novel technique for segmenting breast lesions using a quantization-assisted U-Net approach [48].

III. PROPOSED MODEL

To identify and categorize breast cancer, we have developed a new ELSOSA-BCC algorithm in this work. Also, risk identification of other organs is identified. The proposed ELSOSA-BCC technique encompasses GF-based pre-processing, EfficientNet-B0 feature extraction, SOS-based hyperparameter tuning, and ensemble learning-based classification. The ensemble learning process involves three classifiers namely KELM, DSAE, and BiLSTM models. Fig. 1 represents the workflow of the ELSOSA-BCC approach.

To address this concern, the ELSOSA-BCC approach incorporates a range of strategies. Initially, the ensemble of classifiers is designed with distinct architectures and learning methodologies, aiming to mitigate overfitting by decreasing the probability of all models simultaneously capturing irrelevant variations. This diversity in model designs enhances the ensemble's overall stability and resilience. Furthermore, the integration of precise hyperparameter tuning is an essential step in averting overfitting. By systematically adjusting hyperparameters, the model avoids undue complexity that might lead to overfitting. Techniques like grid search or random search are applied, aiding in identifying optimal

hyperparameters that optimize model performance while ensuring that noise in the data is not overly emphasized.

Additionally, the implementation of cross-validation techniques during both training and assessment contributes to the mitigation of overfitting. Cross-validation evaluates the model's efficacy on distinct data subsets, thereby diminishing the risk of overfitting and ensuring the model's adaptability to unseen data. In conclusion, the ELSOSA-BCC method's reliance on an ensemble of classifiers and meticulous hyperparameter tuning demonstrates a deliberate approach to tackle overfitting. By leveraging the diversity of models and refined hyperparameters, the model aims to strike a balance between capturing meaningful patterns and sidestepping noise, resulting in improved overall generalization capability.

The goal of the study is to investigate ensemble learning strategies to improve the functionality of the breast cancer classification model. Multiple independent classifiers are combined through ensemble learning to produce a more reliable and precise overall prediction. The ensemble learning process will be enhanced using the Symbiotic Organism Search Optimisation (SOS) algorithm. SOS is an optimization method based on symbiosis among organisms that draws inspiration from nature. To improve the classification of breast cancer on histological pictures, the ensemble model's parameters, weights, and architecture are to be optimized using the SOS method. The research attempts to classify breast cancer and also find potential dangers of breast cancer spreading to other bodily organs. This entails examining histopathological scans of various organs (including the heart, liver, lungs, etc.) to look for any anomalies or signs of probable metastases or systemic effects associated with breast cancer. Based on histopathological pictures, the suggested solution should be able to reliably categorize breast cancer subtypes and evaluate the possible hazards to other organs at the same time. To monitor patients and make treatment decisions, the research intends to create a sophisticated and precise tool for identifying and evaluating breast cancer.

In a comparative context, the ELSOSA-BCC method involves a notably higher computational load in comparison to the separate processes of Gabor filtering and ensemble learning. Gabor filtering, which encompasses the analysis of image textures through convolution with specialized filters, can be considered relatively straightforward. Similarly, ensemble learning, which combines predictions from multiple models to enhance accuracy, demands a manageable level of computational resources.

Conversely, the ELSOSA-BCC approach combines Gabor filtering, symbiotic organism search optimization, and ensemble learning into a comprehensive framework. This fusion leads to an intensified computational demand due to the iterative optimization nature of symbiotic organism search and the consolidation of predictions within ensemble learning. Consequently, the utilization of the ELSOSA-BCC method introduces an increased computational load, necessitating a thorough comparative assessment against simpler techniques to validate its intricacies.

Gabor filtering is used as a preprocessing step in the ELSOSA-BCC approach to reduce noise and improve the pertinent texture features in the histopathology images. It entails applying a collection of spatially localized sinusoidal functions known as Gabor filters on an image. Gabor filters are excellent for noise removal and feature extraction in images because they can be used to recover texture information from various frequencies and orientations. The ELSOSA-BCC technique aims to improve the ensemble model's predictive accuracy for classifying breast cancer based on histopathology images. Overall, the ELSOSA-BCC method looks to construct an ensemble model for breast cancer classification by combining Gabor filtering, the EfficientNet-B0 model, and the SOS algorithm. The specific enhancements and performance gains that this ensemble approach has made in comparison to other available techniques in the field will determine the innovation and contribution of the work.

The article introduces the application of Ensemble Learning with the Symbiotic Organism Search Optimization Algorithm (ELSOSA-BCC). ELSOSA-BCC's unique strength lies in its capability to leverage ensemble learning, which amalgamates predictions from diverse algorithms to amplify accuracy and robustness. This methodology proves particularly pertinent in the domain of breast cancer detection, given the need to address subtle variations and intricate patterns within histopathological images comprehensively.

Furthermore, the integration of the Symbiotic Organism Search Optimization Algorithm heightens ELSOSA-BCC's efficacy. This algorithm emulates symbiotic relationships in nature, facilitating dynamic adaptation and optimization of ensemble constituents. Consequently, the ensemble remains agile and proficient in capturing the nuanced attributes of breast cancer pathology.

In contrast to conventional practices that may center on individual algorithms, the Ensemble Learning with Symbiotic Organism Search Optimization Algorithm exploits the collective intelligence of multiple algorithms. This comprehensive strategy aims to surmount the limitations of singular methods and optimize accuracy in breast cancer detection—an essential component of early and precise diagnosis.

A. IMAGE PREPROCESSING

In image processing, a GF is a linear filter utilized for texture synthesis and analysis. It derives from the Gabor wavelet which is a sinusoidal plane wave modulated by the Gaussian function [38]. GFs can be utilized in a variety of applications, comprising texture analysis, edge detection, and feature extraction. They are mostly suitable for studying images that comprise patterns or textures, while the GF is capable of capturing either frequency or orientation data of patterns from the image. To utilize a GF on an image, the image has convolved with a group of Gabor kernels, each one is planned to respond to a specific frequency and orientation. The resultant convolved image is then explored for extracting features or detecting texture and edge [34], [35], [36].

Gabor filtering (GF) plays a vital role as a preprocessing step in a range of image analysis applications, particularly in tasks such as the identification of breast cancer from histopathological images. Its importance arises from its capacity to amplify essential features and patterns present in images, rendering them more suitable for subsequent analytical processes. In essence, Gabor filtering stands as a critical preprocessing measure due to its aptitude for enriching textural attributes, identifying frequency and orientation nuances, mitigating noise interference, and refining image representations for subsequent evaluations. Its integration is indispensable for augmenting the precision and efficacy of breast cancer detection using histopathological images.

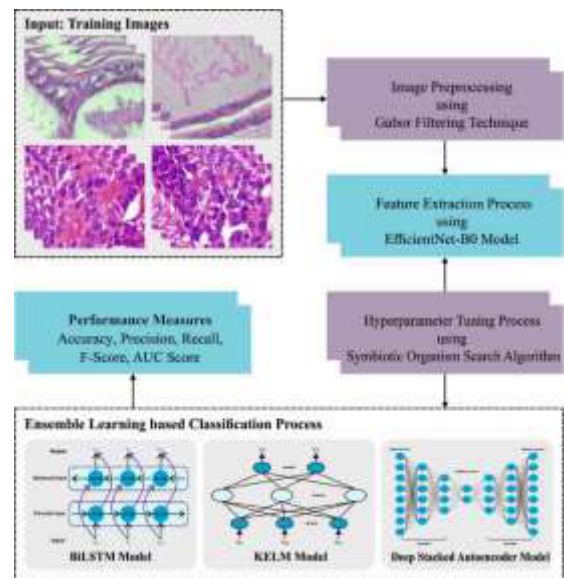


FIGURE 1. Workflow of the ELSOSA-BCC approach.

To sum up, the prospective directions for ELSOSA in Breast Cancer Classification and risk Identification encompass algorithmic advancement, investigation of multi-omics data, bolstering interpretability, rigorous clinical validation, and diversifying its scope to include other medical conditions. These collective endeavors hold the promise of transforming breast cancer diagnosis and risk evaluation, ultimately leading to elevated patient care and better overall outcomes.

B. FEATURE EXTRACTION

For the feature extraction process, the EfficientNet-B0 model is used. The EfficientNet model proposed by Google in 2019 made a great accomplishment in the domain of image classification. To identify sepsis early, this study will use physiological data. Data from patients are used as inputs, including demographics, lab results, and vital signs. To choose the ideal training hyperparameters and probability threshold for the inference phase, we used an LSTM [37]. The EfficientNet model has been used for the ImageNet data and has shown greater performance. The network employs a compound coefficient for scaling the three dimensions of input image

resolution (resolution), network depth (depth), and network width (width) uniformly, thereby, the optimum classification effect can be attained by balancing all the dimensions. In comparison to conventional approaches, these models have a limited amount of parameters and are capable of learning the deep semantic data of images, enriching the efficiency and accuracy of the network. Also, EfficientNet has better transferability.

The EfficientNet includes a multi-model mobile inversion bottleneck (MBConv) with a residual structure. The network model comprises of $k \times k$ DepthwiseConv convolution (Swish and BN, the value k is 3or5), common 1×1 convolutional layer (BN), dropout layer, squeeze, and excitation (SE) model, and 1×1 convolution layer (Swish and Batch Normalization (BN)). These structures may take the count of network parameters while improving the capability of extraction features. Fig. 2 represents the framework of the EfficientNet-B0 method. EfficientNet-b0 is an underlying structure for the lightweight network in image classification. EfficientNet-b0 comprises 9 stages. Stage 1 comprises 3×3 convolutional kernels with a stride of 2. Stages 2 to 8 comprise repetitive stacking of the model, and the column parameter layers characterize the count of times the MB-Conv is reiterated. Stage 9 comprises a fully connected, 1×1 convolution kernel, and average pooling layers. All the MBConv in the table is followed by the number 1 or 6. This number is the magnification factor. Especially, the first convolution layer in the MBConv extends the channel of the input feature map to n times the original. $k3 \times 3$ or $k5 \times 5$ characterizes the size of convolution kernels in the DepthwiseConv layer in MBConv. Resolution signifies the size of the feature map output by these stages. The EfficientNet-b7 sequence of DNN selects the better-suited one in depth (the number of convolutional layers), width (the count of channels of the feature map), and resolution (the size of feature map) based on the width, depth, and resolution of EfficientNet-b0. The fundamental premise is that expanding the depth of the network could

attain rich and complex features. This method is used for other tasks. However the gradient disappears, the training becomes challenging, and the time consumption rises if the network depth is deeper. Assuming that the sampling dataset is comparatively smaller, we applied EfficientNet-b0 as the backbone of the segmentation technique.

The SOS algorithm is used to tune the hyperparameters of the EfficientNet-B0 approach to its best performance. The SOS algorithm, the newest method for tackling optimization problems, was created by Cheng and Prayog in 2014 and was motivated by organism interaction [39]. They rarely exist in solitude since they depend on other species for sustenance and life. These relationships rely upon trust, which can also be called symbiotic relationships. The SOS process starts with the initial population named the ecosystem. A group of organisms was arbitrarily produced in the initial ecosystem, where every organism signifies a solution for the given issue. The SOS method offers a creative approach to simulating biological relationships between the ecosystem’s living things. The SOS technique comprises Parasitism, Mutualism, and Commensalism stages of biological relationships in nature.

1) MUTUALISM

The interaction they share now serves the interests of both organisms. Assume, for example, that honeybees and flowers have a relationship where the bees fly over the bloom to collect nectar needed to produce honey. Additionally, as bees aid in pollination by dispersing pollen, it may benefit flowers. In this work, X_i was an organism that corresponds to the i^{th} individuals in the ecosystem. Then, X_j , who is connected to X_i in the ecosystem, is chosen at random. Finally, in the Mutualism stage, X_i and X_j are upgraded as follows:

$$X_{i\text{new}} = X_i + \text{rand}(0, 1) \times (X_{\text{best}} - \text{Mutual_Vector} \times \text{BF}_1) \tag{1}$$

$$X_{j\text{new}} = X_j + \text{rand}(0, 1) \times (X_{\text{best}} - \text{Mutual_Vector} \times \text{BF}_2) \tag{2}$$

$$\begin{aligned} \text{Mutual_Vector} &= \frac{X_i + X_j}{2} \end{aligned} \tag{3}$$

Random (0, 1) is used to represent the random vector of numbers in the expression. The profit factors of X_i and X_j that show each organism’s return are represented by BF_1 and BF_2 , respectively. Mutual_Vector in Eq. (1) represents the connections between X_i and X_j .

The $\text{Mutual_Vector} \times \text{BF}_2$ in Eqs. (1) & (2) attempts to improve the surviving percentage of living creatures. Each organism must increase its level of compatibility with its environment to survive, according to the Darwinian Theory of the surviving fittest. The X_{best} now denotes the highest level of compatibility.

2) COMMENSALISM

In this stage, the relationships benefit the organism and do not help the other. Consider, for example, the interactions

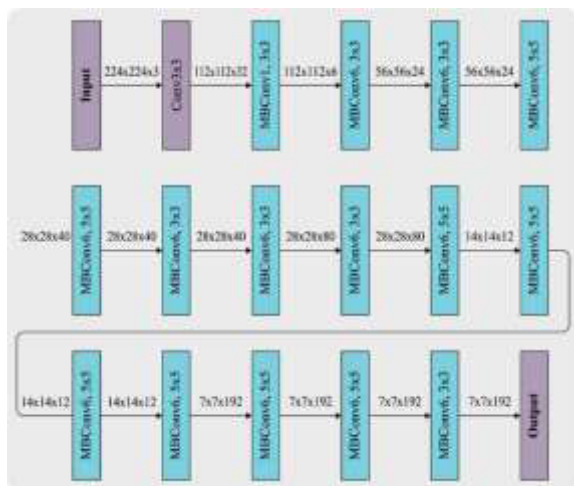


FIGURE 2. The architecture of the EfficientNet-B0 model.

between sharks and sticky fish. Here, the shark receives little to no advantage while the adhesive fish adheres to it and feasts on leftover food. The organism X_j , which is connected to X_i , is carefully selected at random and is present during the Mutualism stage. In these scenarios, X_i aims to make money, yet X_j suffers losses or receives no rewards.

$$X_{new} = X_i + rand(-1, 1) \times (X_{best} - X_j) \quad (4)$$

where $X_{best} - X_j$ signifies the benefit given by X_j for increasing X_i survival.

3) PARASITISM

In this stage, the interaction benefits one organism while causing harm to the other. For example, the blood parasite that causes malaria transfers to the body. Once the parasite has multiplied within the human body, it results in death. In this work, an artificial parasite called ‘‘ParasiteVector’’ is created by X_i , the malaria mosquito. By repeating X_i , the ParasiteVector is created within the search area. The ecology randomly selects X_j to serve as the parasite’s host and help it. The Parasite-Vector attempts to occupy X_j ’s place in the ecology. To assess their competency, X_i and X_j are each given an evaluation. When X_j can fight off the parasite and leave the ecology, they have reached their full potential.

Fitness selection is an important element in the SOS technique. It is possible to assess the quality of a proposed solution using solution encryption. Here, the accuracy values serve as the primary criterion for creating a fitness function.

$$Fitness = max(P) \quad (5)$$

$$P = \frac{TP}{TP + C + FP} \quad (6)$$

According to the term, TP stands for a genuine positive value, and FP for a false positive value.

Algorithm 1 The Pseudocode of the SOS Algorithm

```

Initialized (initial ecosystem, set ecosystem size, and highest iteration)
For counter-l to maximum iteration
  For every organism in the ecosystem
    Mutualism stage based on Eqs (1) and (2)
    The commensalism stage based on Eq. (2)
    Parasitism stage
    Upgrade the better organism
  End For
End For

```

C. ENSEMBLE LEARNING PROCESS

In this work, the ensemble learning process involves three classifiers namely KELM, DSAE, and BiLSTM models. The DL methodology can be utilized in the method that is being described, and a weighted voting mechanism was used to select the best possible result. Prediction class C_k of weighted

voting for each sample was calculated using the number of classes as n and the D base classifier model for voting.

$$c_k = arg\ max_j \sum_{i=1}^D (\Delta_{ji} \times w_i), \quad (7)$$

The binary parameter is denoted in this case by Δ_{ji} . w_i is the weight of the i^{th} base classifier in an ensemble. Once the j^{th} The base classifier has classified the k instance into the j th class, $\Delta_{ji} = 1$; after that, $\Delta_{ji} = 0$.

$$Acc = \frac{\sum_k \{1|c_k \text{ is the true class of instance } k\}}{Size\ of\ test\ instances} \times 100\% . \quad (8)$$

1) KELM MODEL

For training, ANN, the Extreme Learning Machine (ELM) is introduced. The main advantage is that the hidden layer (HL) does not require repeated correction, which speeds up the training process compared to standard ANN [40]. ELM, ANN, and SVM performed inferiorly compared to KELM in their ability to approximate VSM. Additionally, training takes less time than with SVM and ANNs. Maintaining rapid training allows KELM to be retrained in unforeseen situations, improving performance when analyzing LTVS. The ELM technique contains three stages: 1) to implement a random allocation of input weight w_i ; a threshold b_i and HL node parameters; 2) to determine HL’s output matrix H , and 3) to achieve an output weight vector β . The output function has the following representation for the sequence of the N input dataset.

$$H\beta = T \quad (9)$$

In Eq. (9), H denotes the results matrix ($N \times n$) of the HL, β indicates the matrices of output weights ($n \times m$), T shows the goal matrix ($n \times m$) and m represents the random targets. ELM training comprises of minimal norm least square solution of the linear mechanism, which obtains optimum weight $\beta = H^T T$, where $H^T = (H^T H)^{-1} H^T$ shows the Moore-Penrose generalized inverse and it can be formulated as

$$\beta = H^T \left(\frac{I}{C} + H H^T \right)^{-1} T \quad (10)$$

Add positive values $1/C$ to the diagonal of $H H^T$ following the ridge regression theory. Equation (11), where $h(x)$ denotes the sHL feature mapping function, provides the appropriate output function for ELM.

$$f(x) = h(x)\beta = h(x)H^T \left(\frac{I}{C} + H H^T \right)^{-1} T \quad (11)$$

The values of the output function in this work are defined by the kernel function $K(u, v)$. It is possible to supply the kernel function as an inner product. Additionally, while resolving the output function, it is imperative to set multiple HL nodes.

A kernel function was presented to attain the best performance of regression, as follows.

$$f(x) = h(x)H^T \left(\frac{I}{C} + HH^T \right)^{-1} T$$

$$= \begin{Bmatrix} K(x, x_1) \\ \vdots \\ K(x, x_N) \end{Bmatrix} \left(\frac{I}{C} + \Omega_{ELM} \right)^{-1} T \quad (12)$$

$$\Omega_{ELM}(i, j) = h(x_i) \cdot h(x_j) = K(x_i, x_j) \quad (13)$$

where Ω_{ELM} indicates kernel function matrix and $K(u, v)$ denotes kernel function. An RBF is used as a kernel function to increase the generalized capability of KELM. Lastly, it can be noteworthy that before implementing the KELM training, C and γ parameters should be set.

$$K(x_i, x_j) = e^{-\gamma \|x_i - x_j\|^2}, \quad \gamma > 0 \quad (14)$$

2) DSAE MODEL

An auto-encoder (AE) is an FFNN that takes more than one hidden layer (HLs). It is a variety of unsupervised NN, whereas the network efforts to equal output to input vectors are nearly feasible [41]. Additionally, it might be used to create a low-dimensional or high-dimensional representation of the given data. NNs are made to be incredibly adaptable by utilizing unsupervised learning of compression file encoders. These networks are also trained one layer at a time, which reduces the amount of computer resources needed to create an effective model. Once the HLs are lesser dimensional than the output and input layers, afterward network can be utilized for the data encoder (as it permits compression). Multi-layered AEs are trained in sequence, permitting for gradual compressed of data, generating is named stacked AE. Layers HL, input, and output make up the self-encoder technique. The flow table feature vector is:

$$x_i = [x_{i1}, x_{i2}, x_{i3}, \dots, x_{ij}]^T$$

While j represents all flow table features and i is the i^{th} flow table feature vector. The j feature is part of the vector. The flow table based on Eq. (15) uses an input feature vector that has been compressed and encoded in HL.

$$encoder = W_1 x_i + b_1 \quad (15)$$

In which, W_1 stands for the weighted linking of the input layer and HL, the terms x_i and b_1 denote the inputted feature vector of the i^{th} flow table and the bias of the HL neuron, respectively.

Next, the encoder has done and defined the output of HL, and the output layer has been decoder and recreated for producing the output of similar size as the input layer neuron, utilizing Eq. (16):

$$decoder = f(W_2 (encoder)_i + b_2) \quad (16)$$

whereas f refers to the activation function, W_2 denotes the weighted betwixt the output layer and HL, the (*encoder*)

represents stream table feature vector compression by HL coded, and b_2 signifies the bias of the resultant layer neuron.

Lastly, the objective of training the self-encoder method was accomplished by minimizing the loss function utilizing in Eq. (17):

$$loss = \sum_{i=1}^n (x_i - (decoder)_i)^2 \quad (17)$$

whereas n implies the count of the flow table feature vector, x_i signifies the input flow table feature vector, and (*decoder*) represents the flow table feature vector outcome by x_i with the self-encoder method. For accomplishing dimensionality decline and extraction feature if generating the model, it is aimed to exploit the DSAE method. An input layer and HL of self-encoder methods were stacked one on top of the other to create the DSAE method. An HL is produced by each self-encoding method. The compressing abstract feature can then be acquired in its HL, and the HL of the first self-encoder method was used as the input layer of the second self-encoder method. Following the learning of the flow table feature vector by the first self-encoder method, the compressing abstract feature was obtained in its HL. The learning of the second AE method represents that further abstract features are acquired then more compression in its HL.

3) BiLSTM MODEL

The RNN algorithm is used to scrutinize the time series dataset and integrates a return loop permitting to effectively deal with prior experience [42]. On the other hand, RNNs have certain limitations regarding information and memory storage. It cannot learn long-term dependency and might lead to gradient vanishing problems. On account of this, the LSTM was established to overcome the inadequacy of the RNN model. This design was based on the usage of memory cells for storing long-run previous knowledge and regulation of this data through the usage of a gating mechanism. i_t input gate, f_t forget gate, and O_t output gates are the 3 kinds of gates in a conventional LSTM unit. Controlling the state of the memory cell can be attained at every single gate by carrying out sigmoid function operations and pointwise multiplication on the data. Each gate is activated once the input dataset x_t at the present state and the output h_{t-1} from the hidden state of previous layers are entered. The forget gate defines which data needs to be removed and which one needs to be preserved. The sigmoid function transfers data based on the present input x_t and their previously hidden layer h_{t-1} via data from the existing input x_t . Therefore, the output values of the forgetting gate lie within [0,1]. When the value is nearly equal to zero, it indicates that data will be deleted. They are inclined to have further knowledge closer to themselves. The following steps should be considered to calculate the formula for forgetting the gate:

$$f_T = \sigma(W_f \cdot [h_{t-1}, x_t] + b_f) \quad (18)$$

In Eq. (18), W and b are the weight and bias of the gating unit, correspondingly, σ , means the sigmoid activation func-

tion and it is given by the present input x_t and previously hidden layer h_{t-1} as input. The input gate defines which part of the data needs to be updated by changing the value from 0 to 1 through the transformation function. Amongst them, 1 represents significance and 0 signifies insignificance. The input gate can be expressed as follows:

$$i_t = \sigma (W_i \cdot [h_{t-1}, x_t] + b_i) \quad (19)$$

Next, the \tanh function was provided to present input x_t & hidden state h_{t-1} that was attained in advance. Here, the C_t cell state was calculated, and the novel value can be included in the cell states to reflect the change.

$$\hat{C}_t = \tanh (W_c \cdot [h_{t-1}, x_t] + b_c) \quad (20)$$

$$C_t = f_t \odot C_{t-1} + i_t \odot \hat{C}_t \quad (21)$$

where \tanh stands for the hyperbolic tangent's activation function. C_t displays the newly created memory cell, and denotes the dot multiplication operation \odot . The output gate then specifies the next concealed state that will be selected. Next, the novel memory cell C_t and novel hidden state h_t are relocated to the succeeding time step.

$$o_t = \sigma (W_o \cdot [h_{t-1}, p_t] + b_o) \quad (22)$$

$$h_t = o_t \odot \tanh (c_t) \quad (23)$$

Data is generally analyzed in one forward direction by an LSTM. In other words, it is based on past information. Contrarily, BiLSTM was designed with two LSTM layers, one forward and one backward. Forward LSTM might get datasets from past input sequences, whereas the backward LSTM receives datasets from future input sequences, and later output from the hidden layer is fused. In the present time t , the hidden layer h_t of Bi-LSTM encompasses forward \vec{h}_t and backward \overleftarrow{h}_t :

$$h_t = \vec{h}_t \oplus \overleftarrow{h}_t \quad (24)$$

Eq. (24), \oplus indicates the component summation for adding the backward and forward output components. It uses subsequent and previous data while outperforming RNN and LSTM concerning efficacy In the case of BiLSTM.

IV. RESULTS AND DISCUSSION

The histopathological image dataset [43] of 1820 samples with two primary classes as listed in Table 1 is used in this section to test the experimental validity of the ELSOSA-BCC approach. Fig. 3 illustrates the sample images.

The confusion matrices of the ELSOSA-BCC technique are demonstrated in Fig. 4. The results depicted that the ELSOSA-BCC technique has proficiently recognized all the class labels. Although the values of RMSE and STD are small (i.e., close to zero), the ELSOSA-BCC technique was successful in generating a high classification performance throughout 50 runs. Accuracy values for STD were 0.6589.

Performance evaluation of the ELSOSA-BCC technique involves utilizing a range of metrics, including accuracy,

TABLE 1. Details of the dataset.

Category	Class Names	Labels	No. of Images	Total No. of Images in each category
Benign	Adenosis	A	106	588
	Fibroadenoma	F	237	
	Phyllodes Tumor	PT	115	
	Tubular Adenoma	TA	130	
Malignant	Carcinoma	DC	788	1232
	Lobular Carcinoma	LC	137	
	Mucinous Carcinoma	MC	169	
	Papillary Carcinoma	PC	138	
Total Number of Images				1820

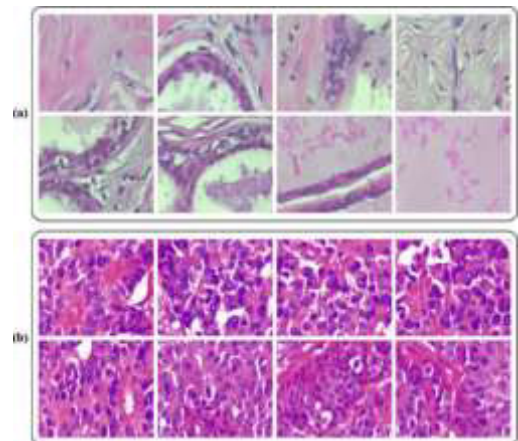


FIGURE 3. Sample images.

precision, recall, F1-score, and AUC-ROC. These metrics collectively offer a comprehensive assessment of the technique's ability to accurately classify both positive and negative instances, providing insights into its overall predictive prowess. Through a rigorous examination involving diverse datasets, meticulous comparisons, and robust statistical analyses, the ELSOSA-BCC technique consistently reveals its supremacy over alternative models. This substantiates its potential for precise breast cancer classification and effective risk identification, establishing its position as an advanced and promising approach in the field.

The overall BC categorization findings are analyzed in Table 2 and Fig. 5 using an 80:20 ratio of TRS and TSS. The outcomes implied that the ELSOSA-BCC approach achieves effective results across all classes. For instance, with 80% of TRS, the ELSOSA-BCC technique gains an average $accu_y$ of 98.75%, $prec_n$ of 93.40%, $reca_l$ of 92.11%, F_{score} of 92.71%, and AUC_{score} of 95.67%. ELSOSA-BCC achieves 20% of

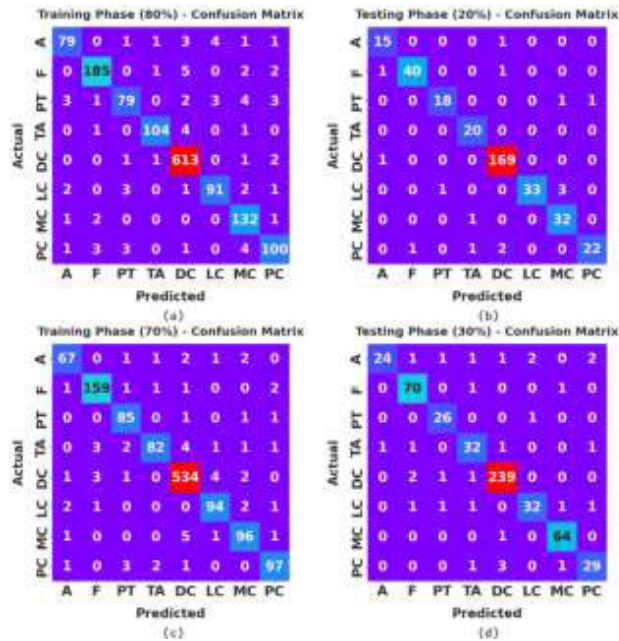


FIGURE 4. Confusion matrices of ELSOSA-BCC method (a-b) TRS/TSS of 80:20 and (c-d) TRS/TSS of 70:30.

TABLE 2. Bc classifier outcome of ELSOSA-BCC approach on 80:20 of TRS/TSS.

Labels	$Accu_y$	$Prec_n$	$Reca_l$	F_{score}	AUC_{score}
Training Phase (80%)					
A	98.76	91.86	87.78	89.77	93.63
F	98.83	96.35	94.87	95.61	97.16
PT	98.35	90.80	83.16	86.81	91.29
TA	99.38	97.20	94.55	95.85	97.16
DC	98.56	97.46	99.19	98.32	98.64
LC	98.90	92.86	91.00	91.92	95.24
MC	98.70	89.80	97.06	93.29	97.96
PC	98.49	90.91	89.29	90.09	94.27
Average	98.75	93.40	92.11	92.71	95.67
Testing Phase (20%)					
A	99.18	88.24	93.75	90.91	96.59
F	99.18	97.56	95.24	96.39	97.46
PT	99.18	94.74	90.00	92.31	94.85
TA	99.45	90.91	100.00	95.24	99.71
DC	98.63	97.69	99.41	98.54	98.67
LC	98.90	100.00	89.19	94.29	94.59
MC	98.63	88.89	96.97	92.75	97.88
PC	98.63	95.65	84.62	89.80	92.16
Average	98.97	94.21	93.65	93.78	96.49

TSS as well as an average $accu_y$ of 98.97%, $prec_n$ of 94.21%, $reca_l$ of 93.65%, F_{score} of 93.78%, and AUC_{score} of 96.49%.

The findings of the overall BC classification are examined in Table 3 and Fig. 6 using a 70:30 ratio of TRS and TSS. The results demonstrated that the ELSOSA-BCC technique achieves effective results across all courses. For example, with 70% of TRS, the ELSOSA-BCC approach attains an average $accu_y$ of 98.82%, $prec_n$ of 93.91%, $reca_l$ of 93.54%, F_{score} of 93.69%, and 96.40%. Moreover, with 30% of TSS, the ELSOSA-BCC algorithm reaches an average $accu_y$ of

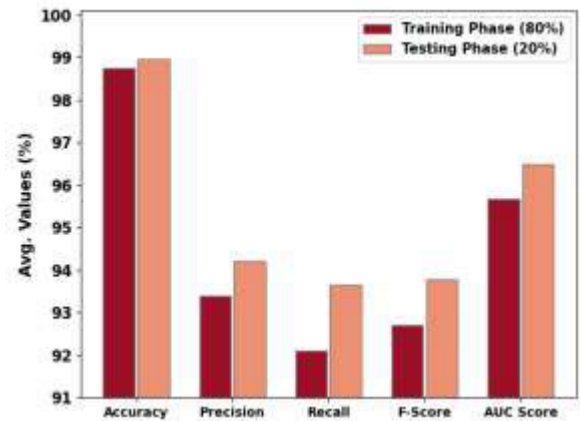


FIGURE 5. Average outcome of ELSOSA-BCC approach on 80:20 of TRS/TSS.

TABLE 3. Bc classifier outcome of ELSOSA-BCC approach on 70:30 TRS/TSS.

Labels	$Accu_y$	$Prec_n$	$Reca_l$	F_{score}	AUC_{score}
Training Phase (70%)					
A	98.98	91.78	90.54	91.16	95.02
F	98.98	95.78	96.36	96.07	97.87
PT	99.14	91.40	96.59	93.92	97.96
TA	98.74	95.35	87.23	91.11	93.45
DC	98.04	97.45	97.98	97.71	98.03
LC	98.98	93.07	94.00	93.53	96.70
MC	98.74	92.31	92.31	92.31	95.81
PC	98.98	94.17	93.27	93.72	96.38
Average	98.82	93.91	93.54	93.69	96.40
Testing Phase (30%)					
A	98.35	96.00	75.00	84.21	87.40
F	98.72	93.33	97.22	95.24	98.08
PT	99.27	89.66	96.30	92.86	97.86
TA	98.35	86.49	88.89	87.67	93.95
DC	98.17	97.55	98.35	97.95	98.19
LC	98.53	91.43	86.49	88.89	92.95
MC	99.27	95.52	98.46	96.97	98.92
PC	98.35	87.88	85.29	86.57	92.26
Average	98.63	92.23	90.75	91.29	94.95

98.63%, $prec_n$ of 92.23%, $reca_l$ of 90.75%, F_{score} of 91.29%, and AUC_{score} of 94.95%.

A comparison of TACY and VACY for the ELSOSA-BCC technique on BC performance is presented in Figure 7. A comparison of the ELSOSA-BCC approach with the traditional approach shows increased VACY and TACY values with ELSOSA-BCC. There seems to be a maximum TACY outcome for the ELSOSA-BCC method.

Fig. 8 shows the performance of the ELSOSA-BCC technique in terms of TLOS and VLOS. With minimal TLOS and VLOS values, ELSOSA-BCC performed better than conventional methods. It is noteworthy that the ELSOSA-BCC method has had an impact on reducing VLOS.

As illustrated in Figure 9, TA clear precision-recall testing was performed on the ELSOSA-BCC method in the test database. Each class label's precision-recall values were improved by the ELSOSA-BCC method.

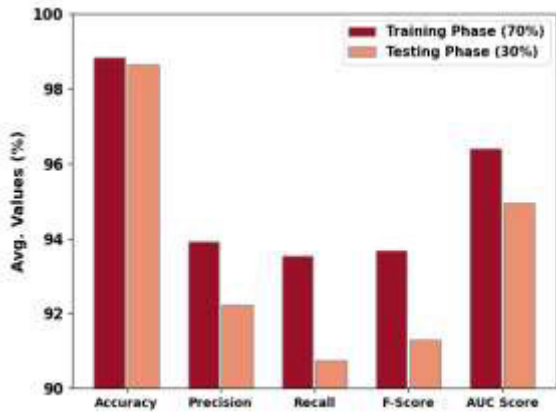


FIGURE 6. The average outcome of the ELSOSA-BCC method on 70:30 of TRS/TSS.

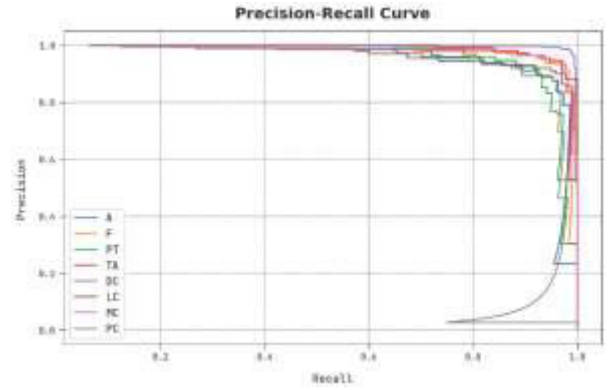


FIGURE 9. The precision-recall outcome of the ELSOSA-BCC method.

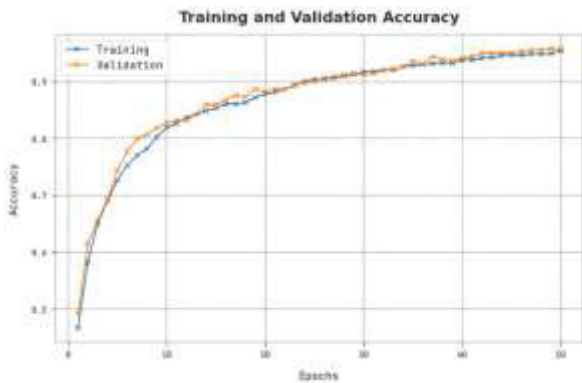


FIGURE 7. TACY and VACY outcome of the ELSOSA-BCC approach.

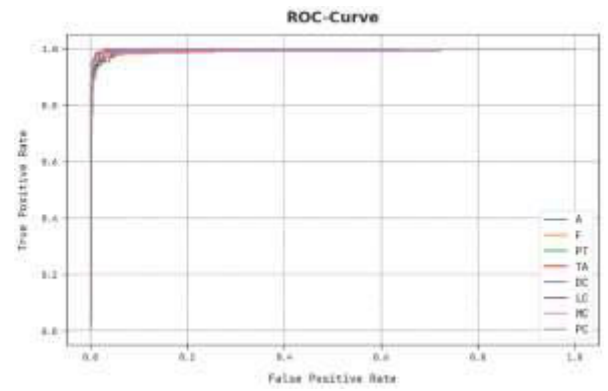


FIGURE 10. ROC curve outcome of ELSOSA-BCC method.



FIGURE 8. TLOS and VLOS outcome of ELSOSA-BCC approach.

TABLE 4. Comparative analysis of the ELSOSA-BCC method with other approaches.

Methods	$Accu_y$	$Prec_n$	$Reca_l$	F_{score}
KNN	75.97	62.32	83.79	82.35
NB	78.62	82.06	83.59	87.14
Discrete Transform	85.19	83.70	81.51	84.55
SVM	84.83	87.28	87.75	81.63
DL Model	94.89	87.42	87.19	81.93
CSSADTL-BCC	98.59	92.67	91.53	91.91
ELSOSA-BCC	98.97	94.21	93.65	93.78

According to Fig. 10, the detailed ROC analysis of the ELSOSA-BCC methodology under the test database can be found here. The results demonstrated that the ELSOSA-BCC technique is capable of classifying different categories.

In Table 4 and Fig. 11, a brief comparative study of the ELSOSA-BCC method with current approaches takes place [44], [45]. The algorithm’s overall performance, separate from the classes, is demonstrated by the performance metrics

above. The outcomes indicate that the KNN and NB approach attain reduced classification results while the DT and SVM models have managed to obtain slightly improved performance. Then, the DL model has accomplished moderate performance over other models. However, the ELSOSA-BCC technique showed maximum performance with an $accu_y$ of 98.97%, $prec_n$ of 94.21%, $reca_l$ of 93.65%, and F_{score} of 93.78%. These results pointed out the supremacy of the ELSOSA-BCC algorithm over other existing models. Correctness of the outcomes produced by optimization utilizing

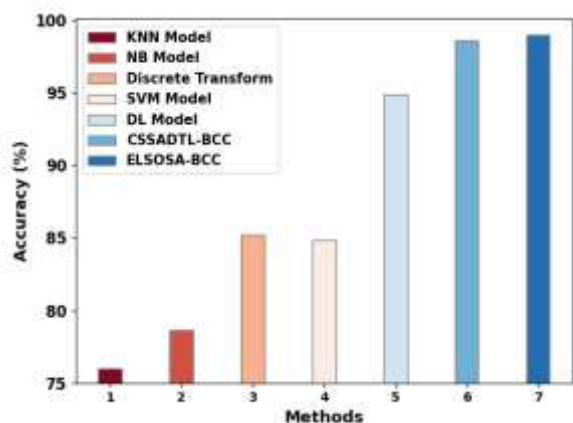


FIGURE 11. Accuracy analysis of the ELSOSA-BCC approach with other algorithms.

the suggested ELSOSA-BCC approach in comparison to other methods. This outcome highlights the excellence of the suggested methodology even more accurately based on different parameters during result analysis $Accu_y$, $Prec_n$, $Recal_1$, and F_{score} . comparison is classifier-based, Even less specific features, known as discrete cosine transform (DCT) features, are related to representations of textures and colors.

V. CONCLUSION AND FUTURE WORKS

We have devised a novel means of detecting and classifying breast cancer using the ELSOSA-BCC innovative technique. An ELSOSA-BCC technique is presented that incorporates preprocessing based on GFs, feature extraction based on EfficientNet-B0, hyperparameter tuning based on SOSs, and ensemble classification based on ensemble learning. KELM, DSAE, and BiLSTM models are utilized in the ensemble learning process. Medical datasets are used to test the simulation results of the ELSOSA-B CC method. The experimental outcomes stated that the ELSOSA-BCC technique reaches improved performance over other models. The research focuses on how breast cancer swiftly affects other organs. Therefore, the ELSOSA-BCC technique is found to be an effective tool for automated breast cancer classification. In the future, deep instance segmentation models will be derived to improve the detection rate of the ELSOSA-BCC method.

VI. FUTURE WORK

The application of Ensemble Learning with Symbiotic Organism Search Optimization Algorithm (ELSOSA) has predominantly been observed in breast cancer prediction scenarios. It's crucial to recognize that diverse types of cancer prediction tasks demand distinct expertise and meticulous assembly of datasets. Although there may be a lack of documented cases showcasing ELSOSA's utilization in various cancer predictions, the underlying concept of combining ensemble learning with optimization holds promise for augmenting predictive precision in numerous medical contexts, encompassing cancer prognosis.

In the domain of other cancer prediction, researchers have harnessed an array of machine learning and AI techniques, including the incorporation of ensemble methodologies. Several prevalent categories of cancer prediction tasks encompass:

- 1) **Lung Cancer Prediction:** The anticipation of lung cancer entails the examination of medical imaging data, such as CT scans, and pertinent patient details to prognosticate the presence of lung cancer. The integration of ensemble methods holds the potential to elevate prediction accuracy.
- 2) **Prostate Cancer Prediction:** Analogous to breast cancer, predictive models can be constructed using patient demographics, genetic information, and imaging findings to foresee the probability of prostate cancer.
- 3) **Colorectal Cancer Prediction:** Foreseeing colorectal cancer might entail the scrutiny of colonoscopy images, genetic indicators, and patient medical history to assess the susceptibility to this type of cancer.
- 4) **Ovarian Cancer Prediction:** In ovarian cancer prediction, data encompassing genetic profiles, imaging findings, and clinical particulars could be employed to appraise the likelihood of ovarian cancer.
- 5) **Brain Cancer Prediction:** The realm of brain cancer prediction often involves the analysis of MRI or CT images alongside clinical information to pinpoint potential instances of brain tumors.
- 6) **Skin Cancer Prediction:** Predictive models based on machine learning have been leveraged to predict skin cancer via the evaluation of images depicting moles or lesions. Ensembling techniques hold the potential to refine such models.
- 7) **Leukemia Prediction:** The prognostication of leukemia might necessitate the analysis of blood cell counts, genetic markers, and diverse medical data. Ensemble methods stand to augment the precision of diagnosis.

REFERENCES

- [1] N. M. U. Din, R. A. Dar, M. Rasool, and A. Assad, "Breast cancer detection using deep learning: Datasets, methods, and challenges ahead," *Comput. Biol. Med.*, vol. 149, Oct. 2022, Art. no. 106073.
- [2] K. Yu, L. Tan, L. Lin, X. Cheng, Z. Yi, and T. Sato, "Deep-learning-empowered breast cancer auxiliary diagnosis for 5GB remote e-health," *IEEE Wireless Commun.*, vol. 28, no. 3, pp. 54–61, Jun. 2021.
- [3] M. Liu, L. Hu, Y. Tang, C. Wang, Y. He, C. Zeng, K. Lin, Z. He, and H. Huo, "A deep learning method for breast cancer classification in the pathology images," *IEEE J. Biomed. Health Informat.*, vol. 26, no. 10, pp. 5025–5032, Oct. 2022.
- [4] S. Khairi, M. Bakar, M. Alias, S. Bakar, C.-Y. Liong, N. Rosli, and M. Farid, "Deep learning on histopathology images for breast cancer classification: A bibliometric analysis," *Healthcare*, vol. 10, no. 1, p. 10, Dec. 2021.
- [5] C. Chen, S. Zheng, L. Guo, X. Yang, Y. Song, Z. Li, Y. Zhu, X. Liu, Q. Li, H. Zhang, N. Feng, Z. Zhao, T. Qiu, J. Du, Q. Guo, W. Zhang, W. Shi, J. Ma, and F. Sun, "Identification of misdiagnosis by deep neural networks on a histopathologic review of breast cancer lymph node metastases," *Sci. Rep.*, vol. 12, no. 1, pp. 1–10, Aug. 2022.
- [6] E. M. Senan, F. W. Alsaade, M. I. A. Al-Mashhadani, H. H. Theyazn, and W. H. Al-Adhaileh, "Classification of histopathological images for early detection of breast cancer using deep learning," *J. Appl. Sci. Eng.*, vol. 24, no. 3, pp. 323–329, 2021.

- [7] A. B. Nassif, M. A. Talib, Q. Nasir, Y. Afadar, and O. Elgendy, "Breast cancer detection using artificial intelligence techniques: A systematic literature review," *Artif. Intell. Med.*, vol. 127, May 2022, Art. no. 102276.
- [8] J. Yang, J. Ju, L. Guo, B. Ji, S. Shi, Z. Yang, S. Gao, X. Yuan, G. Tian, Y. Liang, and P. Yuan, "Prediction of HER2-positive breast cancer recurrence and metastasis risk from histopathological images and clinical information via multimodal deep learning," *Comput. Struct. Biotechnol. J.*, vol. 20, pp. 333–342, Jan. 2022.
- [9] P. Gamble, R. Jaroensri, H. Wang, F. Tan, M. Moran, T. Brown, I. Flament-Auvigne, E. A. Rakha, M. Toss, D. J. Dabbs, P. Regitnig, N. Olson, J. H. Wren, C. Robinson, G. S. Corrado, L. H. Peng, Y. Liu, C. H. Mermel, D. F. Steiner, and P.-H.-C. Chen, "Determining breast cancer biomarker status and associated morphological features using deep learning," *Commun. Med.*, vol. 1, no. 1, pp. 1–12, Jul. 2021.
- [10] Y. Wang, B. Acs, S. Robertson, B. Liu, L. Solorzano, C. Wählby, J. Hartman, and M. Rantalainen, "Improved breast cancer histological grading using deep learning," *Ann. Oncol.*, vol. 33, no. 1, pp. 89–98, Jan. 2022.
- [11] M. Moscalu, R. Moscalu, C. G. Dascalu, V. Tarca, E. Cojocaru, I. M. Costin, E. Tarca, and I. L. Șerban, "Histopathological images analysis and predictive modeling implemented in digital pathology—Current affairs and perspectives," *Diagnostics*, vol. 13, no. 14, p. 2379, Jul. 2023.
- [12] N. Melarkode, K. Srinivasan, S. M. Qaisar, and P. Plawiak, "AI-powered diagnosis of skin cancer: A contemporary review, open challenges and future research directions," *Cancers*, vol. 15, no. 4, p. 1183, Feb. 2023.
- [13] A.-G. Goubet, "Could the tumor-associated microbiota be the new multifaceted player in the tumor microenvironment?" *Frontiers Oncol.*, vol. 13, May 2023, Art. no. 1185163.
- [14] A. A. Alhussan, M. M. Eid, S. K. Towfek, and D. S. Khafaga, "Breast cancer classification depends on the dynamic dipper throated optimization algorithm," *Biomimetics*, vol. 8, no. 2, p. 163, Apr. 2023.
- [15] O. Stephen and M. Sain, "Using deep learning with Bayesian–Gaussian inspired convolutional neural architectural search for cancer recognition and classification from histopathological image frames," *J. Healthcare Eng.*, vol. 2023, pp. 1–9, Feb. 2023.
- [16] N. Ahmad, S. Asghar, and S. A. Gillani, "Transfer learning-assisted multi-resolution breast cancer histopathological images classification," *Vis. Comput.*, vol. 38, no. 8, pp. 2751–2770, Aug. 2022.
- [17] S. Singh and R. Kumar, "Breast cancer detection from histopathology images with deep inception and residual blocks," *Multimedia Tools Appl.*, vol. 81, no. 4, pp. 5849–5865, Feb. 2022.
- [18] D. Ravi, C. Wong, F. Deligianni, M. Berthelot, J. Andreu-Perez, B. Lo, and G.-Z. Yang, "Deep learning for health informatics," *IEEE J. Biomed. Health Informat.*, vol. 21, no. 1, pp. 4–21, Jan. 2017.
- [19] B. Jena, S. Saxena, G. K. Nayak, L. Saba, N. Sharma, and J. S. Suri, "Artificial intelligence-based hybrid deep learning models for image classification: The first narrative review," *Comput. Biol. Med.*, vol. 137, Oct. 2021, Art. no. 104803.
- [20] R. Gowthaman, K. Jayavignesh, V. Jeevanantham, and K. S. Veeradanya, "Brain neoplasm classification & detection of accuracy on MRI images," *Int. J. Orange Technol.*, vol. 4, no. 5, pp. 25–44, 2022.
- [21] M. M. Fadel, N. G. Elseddeq, R. Arnous, Z. H. Ali, and A. I. Eldesouky, "A fast accurate deep learning framework for prediction of all cancer types," *IEEE Access*, vol. 10, pp. 122586–122600, 2022, doi: 10.1109/ACCESS.2022.3222365.
- [22] D. Devarajan, D. S. Alex, T. R. Mahesh, V. V. Kumar, R. Aluvalu, V. U. Maheswari, and S. Shitharth, "Cervical cancer diagnosis using intelligent living behavior of artificial jellyfish optimized with artificial neural network," *IEEE Access*, vol. 10, pp. 126957–126968, 2022, doi: 10.1109/ACCESS.2022.3221451.
- [23] P. Liu, M. Zhang, X. Gao, B. Li, and G. Zheng, "Joint lymphoma lesion segmentation and prognosis prediction from baseline FDG-PET images via multitask convolutional neural networks," *IEEE Access*, vol. 10, pp. 81612–81623, 2022, doi: 10.1109/ACCESS.2022.3195906.
- [24] K. C. Burçak, Ö. K. Baykan, and H. Uguz, "A new deep convolutional neural network model for classifying breast cancer histopathological images and the hyperparameter optimisation of the proposed model," *J. Supercomput.*, vol. 77, no. 1, pp. 973–989, Jan. 2021.
- [25] R. Yan, F. Ren, Z. Wang, L. Wang, T. Zhang, Y. Liu, X. Rao, C. Zheng, and F. Zhang, "Breast cancer histopathological image classification using a hybrid deep neural network," *Methods*, vol. 173, pp. 52–60, Feb. 2020.
- [26] N. Routray, S. K. Rout, and B. Sahu, "Breast cancer prediction using deep learning technique RNN and GRU," in *Proc. 2nd Int. Conf. Comput. Sci., Eng. Appl. (ICCSEA)*, Sep. 2022, pp. 1–5.
- [27] S. K. Rout, B. Sahu, G. B. Regulwar, and V. Kavidevi, "Deep learning in early prediction of sepsis and diagnosis," in *Proc. Int. Conf. Advancement Technol. (ICONAT)*, Jan. 2023, pp. 1–5.
- [28] F. A. Zeiser, C. A. da Costa, G. D. O. Ramos, H. C. Bohn, I. Santos, and A. V. Roehle, "DeepBatch: A hybrid deep learning model for interpretable diagnosis of breast cancer in whole-slide images," *Exp. Syst. Appl.*, vol. 185, Dec. 2021, Art. no. 115586.
- [29] M. Toğaçar, K. B. Özkurt, B. Ergen, and Z. Cömert, "BreastNet: A novel convolutional neural network model through histopathological images for the diagnosis of breast cancer," *Phys. A, Stat. Mech. Appl.*, vol. 545, May 2020, Art. no. 123592.
- [30] S. Taheri and Z. Golrizkhatami, "Magnification-specific and magnification-independent classification of breast cancer histopathological image using deep learning approaches," *Signal, Image Video Process.*, vol. 17, no. 2, pp. 583–591, 2022.
- [31] M. Swain, S. Kisan, J. Moy, M. Supramaniam, S. Nandan, N. Jhanjhi, and A. Abdullah, "Hybridized machine learning based fractal analysis techniques for breast cancer classification," *Int. J. Adv. Comput. Sci. Appl.*, vol. 11, no. 10, pp. 179–184, 2020.
- [32] S. K. Lakshmanaprabu, S. N. Mohanty, K. Shankar, N. Shankar, and G. Ramirez, "Optimal deep learning model for classification of lung cancer on CT images," *Future Gener. Comput. Syst.*, vol. 92, pp. 374–382, Mar. 2019.
- [33] B. Sahu, S. Mohanty, and S. Rout, "A hybrid approach for breast cancer classification and diagnosis," *EAI Endorsed Trans. Scalable Inf. Syst.*, vol. 6, no. 20, pp. 1–8, 2019.
- [34] B. Sahu, S. Dash, S. N. Mohanty, and S. K. Rout, "Ensemble comparative study for diagnosis of breast cancer datasets," *Int. J. Eng. Technol.*, vol. 7, p. 281, Oct. 2018.
- [35] S. A. Althubiti, S. Paul, R. Mohanty, S. N. Mohanty, F. Alenezi, and K. Polat, "Ensemble learning framework with GLCM texture extraction for early detection of lung cancer on CT images," *Comput. Math. Methods Med.*, vol. 2022, pp. 1–14, Jun. 2022.
- [36] S. Mohapatra, S. Satpathy, and S. N. Mohanty, "A comparative knowledge base development for cancerous cell detection based on deep learning and fuzzy computer vision approach," *Multimedia Tools Appl.*, vol. 81, no. 17, pp. 24799–24814, Jul. 2022.
- [37] S. K. Rout, B. Sahu, A. Panigrahi, B. Nayak, and A. Pati, "Early detection of sepsis using LSTM neural network with electronic health record," in *Ambient Intelligence in Health Care*. Singapore: Springer, 2022, pp. 201–207.
- [38] V. Dakshayani, G. R. Locharla, P. Plawiak, V. Datti, and C. Karri, "Design of a Gabor filter-based image denoising hardware model," *Electronics*, vol. 11, no. 7, p. 1063, Mar. 2022.
- [39] M. J. Gordanloo and F. S. Gharehchopogh, "A hybrid OBL-based firefly algorithm with symbiotic organisms search algorithm for solving continuous optimization problems," *J. Supercomput.*, vol. 78, no. 3, pp. 3998–4031, Feb. 2022.
- [40] W. M. Villa-Acevedo, J. M. López-Lezama, D. G. Colomé, and J. Cepeda, "Long-term voltage stability monitoring of power system areas using a kernel extreme learning machine approach," *Alexandria Eng. J.*, vol. 61, no. 2, pp. 1353–1367, Feb. 2022.
- [41] A. L. Yaser, H. M. Mousa, and M. Hussein, "Improved DDoS detection utilizing deep neural networks and feedforward neural networks as autoencoder," *Future Internet*, vol. 14, no. 8, p. 240, Aug. 2022.
- [42] P. K. Shrivastava, M. Sharma, P. Sharma, and A. Kumar, "HCBiLSTM: A hybrid model for predicting heart disease using CNN and BiLSTM algorithms," *Meas., Sensors*, vol. 25, Feb. 2023, Art. no. 100657.
- [43] F. A. Spanhol, L. S. Oliveira, C. Petitjean, and L. Heutte, "A dataset for breast cancer histopathological image classification," *IEEE Trans. Biomed. Eng.*, vol. 63, no. 7, pp. 1455–1462, Jul. 2016.
- [44] K. Shankar, A. K. Dutta, S. Kumar, G. P. Joshi, and I. C. Doo, "Chaotic sparrow search algorithm with deep transfer learning enabled breast cancer classification on histopathological images," *Cancers*, vol. 14, no. 11, p. 2770, Jun. 2022.
- [45] M. A. Hamza, H. A. Mengash, M. K. Nour, N. Alasmari, A. S. A. Aziz, G. P. Mohammed, A. S. Zamani, and A. A. Abdelmageed, "Improved bald eagle search optimization with synergic deep learning-based classification on breast cancer imaging," *Cancers*, vol. 14, no. 24, p. 6159, Dec. 2022.

- [46] R. Irfan, A. A. Almazroi, H. T. Rauf, R. Damaševičius, E. A. Nasr, and A. E. Abdelgawad, "Dilated semantic segmentation for breast ultrasonic lesion detection using parallel feature fusion," *Diagnostics*, vol. 11, no. 7, p. 1212, Jul. 2021.
- [47] S. Maqsood, R. Damaševičius, and R. Maskeliūnas, "TTCNN: A breast cancer detection and classification towards computer-aided diagnosis using digital mammography in early stages," *Appl. Sci.*, vol. 12, no. 7, p. 3273, Mar. 2022.
- [48] T. Meraj, W. Alosaimi, B. Alouffi, H. T. Rauf, S. A. Kumar, R. Damasevicius, and H. Alyami, "A quantization assisted U-Net study with ICA and deep features fusion for breast cancer identification using ultrasonic data," *PeerJ Comput. Sci.*, vol. 7, p. e805, Dec. 2021.



SANDEEP KUMAR PANDA is currently a Professor and the Head of Department with the Department of Artificial Intelligence and Data Science, Faculty of Science and Technology (IcfaiTech), ICFAI Foundation for Higher Education (Deemed to be University), Hyderabad, Telangana, India. He has published 50 papers in international journals, international conferences, and book chapters in repute. He has 17 Indian patents on his credit. He has six edited books entitled *Bitcoin and Blockchain: History and Current Applications* (CRC Press, USA), *Blockchain Technology: Applications and Challenges* (Springer, ISRL), *AI and ML in Business Management: Concepts, Challenges, and Case Studies* (CRC Press, USA), *The New Advanced Society: Artificial Intelligence and Industrial Internet of Things Paradigm* (Wiley Press, USA), *Recent Advances in Blockchain Technology: Real-World Applications* (Springer, ISRL), and *Metaverse and Immersive Technologies: An Introduction to Industrial Business and Social Applications*, (Wiley Press, USA) in his credit. He has ten lakhs seed money projects from IFHE. His research interests include blockchain technology, the Internet of Things, AI, and cloud computing. He received the Research and Innovation of the Year Award 2020 from MSME, Government of India, and DST, Government of India, New Delhi, in 2020; and the Research Excellence Award from Brand Honchos, in 2022. He is a Reviewer of IEEE Access. His professional affiliations are MIEEE, MACM, and LMAIENG.



NALINIKANTA ROUTRAY received the M.Tech. degree from Utkal University, Bhubaneswar, Odisha, India. He has joined as a Research Scholar with GIET University, Gunupur, Odisha. His research interests include deep learning and machine learning.



SAROJA KUMAR ROUT received the M.Tech. degree in computer science (CS) from Utkal University, in 2007, and the Ph.D. degree in CS from Siksha 'O' Anusandhan University, in 2018, for work in the field of wireless sensor networks. He is currently an Associate Professor with the Department of Information Technology, Vardhaman College of Engineering (Autonomous), Hyderabad, India. He has contributed more than 60 research-level papers to many national and international journals and conferences. He has eight Indian patents. His research interests include sensor networks, machine learning, cloud computing, and health informatics.



BANDITA SAHU received the M.Tech. degree from the National Institute of Technology (NIT), Rourkela, India, in 2015, and the Ph.D. degree from the Department of Computer Science and Engineering, Veer Surendra Sai University of Technology (VSSUT) (A Unitary Technical University, Established by Government of Odisha), Burla, Odisha, India. She is currently an Associate Professor with the Department of Computer Science and Engineering, GIET University, Gunupur, Odisha. She has 18 years of teaching experience. She has published more than 25 papers in top international journals and conference proceedings. She has guided seven M.Tech. scholars. For her credit six Ph.D. scholars are currently working under her able guidance. Her current research interests include intelligent robotics, machine intelligence, and cluster computing.



DEEPTHI GODAVARTHI received the Ph.D. degree from Andhra University, Andhra Pradesh, India, in 2022. She is currently an Assistant Professor with the School of Computer Science and Engineering, VIT-AP University, Amaravati, Andhra Pradesh. Her research interests include AI, NLP, computer vision, and block chain technologies.

...